

Simulating a Delayed Injection Electrodes to Improve the Mass Detection Range of a Fourier Transform Ion Cyclotron Resonance Mass Spectrometer

Myoung Choul Choi,* A Leum Park, Kyu Hwan Park, and Hyun Sik Kim*

Korea Basic Science Institute, Ochang 363-883, Korea. *E-mail: cmc@kbsi.re.kr
Received July 26, 2012, Accepted October 9, 2012

Key Words : FTICR MS, Ion guide, Time-of-flight effect, Delayed injection, ICR cell

A Fourier transform ion cyclotron resonance mass spectrometer (FT-ICR MS)¹ with a high-efficiency ion-guide device was developed at the Korea Basic Science Institute (KBSI).² Most FT-ICR MS with an external source accumulate ions and transmit them to an ion cyclotron resonance (ICR) trap^{1,13} through long ion guide optics. During transmission through the ion guide, ions are dispersed according to their mass and reach the ICR trap at different times according to their velocity, which is time-of-flight induced mass discrimination. Several approaches have attempted to compensate for this. One is to use a gated deceleration potential in a matrix-assisted laser desorption/ionization (MALDI) source to attenuate the translational velocities and internal energies of the desorbed ions.³ The other is to use a radio frequency (rf) ion guide, which is divided into 19 segments.⁴ But, “gated trapping” is simpler and common method for catching ions generated externally or in-field at the ICR trap. Gated trapping does not catch ions over a wide velocity range.⁵ This method has been improved in in-field MALDI source FTMS, because MALDI-generated ions make coupling difficult as the ICR trap requires efficient trapping of low-energy ions. To minimize the kinetic energy of ions, a gated retarding potential was used.⁶⁻⁹ Even with these improvements, gated trapping has not been able to catch ions over a wide mass range. Frankevich and Zenobi presented a simple method for ion deceleration in an open ICR trap.¹⁰ This method applied an electrostatic deceleration potential of up to 100 V to the front cylinder electrode of the open trap. When ions reached 100 V, the potential was set to zero, drastically decreasing ion velocity. We applied this strategy to an electrospray ionization (ESI) source of the FTICR MS in order to improve the mass discrimination at the rf ion guide. A major shortcoming in Frankevich’s method is that the deceleration voltage is applied only at the front cylinder trap, making the deceleration region too small to control a wide mass range of ions. To increase the mass detection range in this study, a delayed-ion-injection device (DIID) was introduced in front of the ICR trap, which will be very simple way to control the ion’s dispersion.

The new electrode (DIID) is 150 mm long and has been designed to be mounted in front of the ICR trap to decelerate the velocity of ions at the front of the ion guide stream. This DIID has a plateau potential field of almost 150 mm. This square-like potential field can reduce the velocity of fast ions

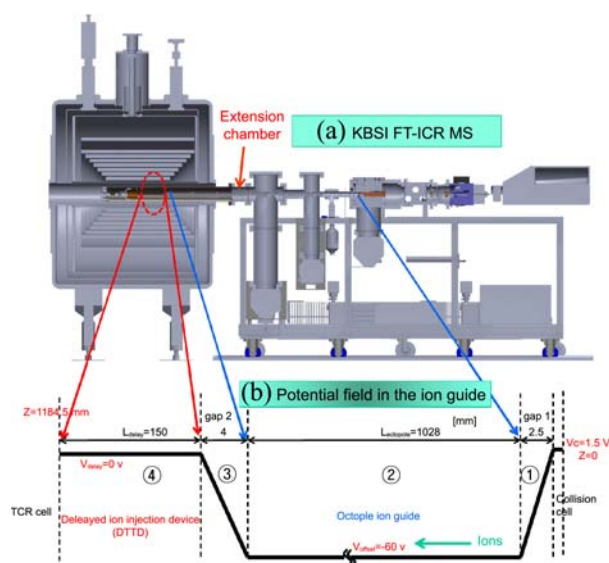


Figure 1. (a) KBSI FTICR MS; 1 (b) potential fields from the extraction lens of the collision cell to the ICR trap.

over a relatively long time and space. When fast, light ions arrive and enter the front of the DIID, ions are decelerated by the potential gradient at “gap 2” in Figure 1, where the potential level is constant at the DIID.

Thus, ions travel toward the ICR trap at a uniform, slow velocity; over time, the potential level of the DIID is switched to a lower potential value. Light ions in the DIID maintain a constant velocity while slower, heavy ions arriving at the front of the DIID experience a lower potential level. Therefore, high-mass ions can move faster. This effect can cause an over-lap between the low mass region and the high mass region at the ICR trap that can efficiently improve the detection mass range. Here, we report simulation results for a newly designed DIID to control the ion energy and improve the mass-detection range of the FT-ICR MS technique.

Theory

A simple relationship between ion position (z) and arrival time (T) at the ICR trap with respect to the potential level of the DIID was constructed. As shown in Figure 1(b), potential fields were presumed to extend from the extraction lenses of the collision cell to the ICR trap, including the

DIID. Between each collision cell, the gap potential fields of an octopole ion guide^{2,12} and an ICR trap were assumed to be linear to simplify the equation. From these assumptions, equations of time and position were developed, and are shown below:

$$T = \sqrt{\frac{m}{e}} \left(\frac{\sqrt{2} gap_1}{\sqrt{V1}} + \frac{L_{octopole}}{\sqrt{2V1}} + \frac{gap_2 \sqrt{2}}{\sqrt{V1} + \sqrt{V2}} + \frac{L_{delay}}{\sqrt{2V2}} \right) \quad (1)$$

$$z = \sqrt{V2} \left(\frac{t \sqrt{2}}{\sqrt{m/e}} - \frac{L_{octopole} + 2gap_1}{\sqrt{V1}} - \frac{2gap_2}{\sqrt{V1} + \sqrt{V2}} \right)$$

m : ion mass

e : electron charge

V_{offset} : offset voltage of the octopole ion guide

V_c : offset voltage of the collision cell

V_{delay} : offset voltage of the DIID

$V1$: ion kinetic energy after gap 1 ($V1 = V_c - V_{offset}$)

$V2$: ion kinetic energy after gap 2. ($V2 = V_c - V_{delay}$)

$L_{octopole}$: length of the octopole ion guide

L_{delay} : length of the DIID

T : arrival time at the front of the ICR trap

z : position in the DIID

In Figure 2, z -positions are plotted against ion mass using Eq. (1). The V_c was 1.5 V DC, and V_{offset} was -60 V DC. V_{delay} , the potential level at the DIID (④ in Figure 1), applied a step-down voltage with time (Figure 3), causing the kinetic energy between low-mass and high-mass ions to differ. Two control parameters were used to control the ion kinetic energy: V_{delay} and t_{off} . As shown in Figure 2, V_{delay} controls the ion kinetic energy on the DIID by deceleration; therefore,

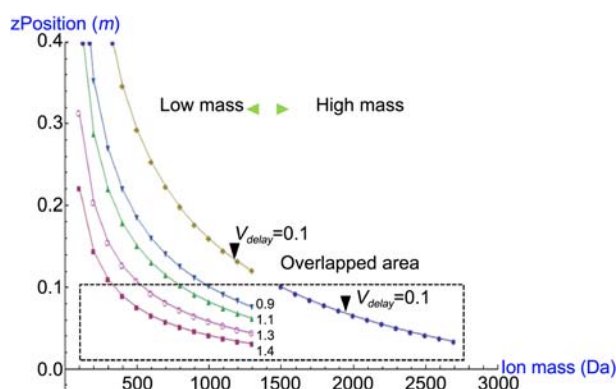


Figure 2. Plot of z -position of each ion mass at $t = 0.0006$ s with $V2 = 0.2$ – 1.4 ; ($V_c = 1.5$ V, $V_{offset} = -60$ V, $V_{delay} = 0$ V).

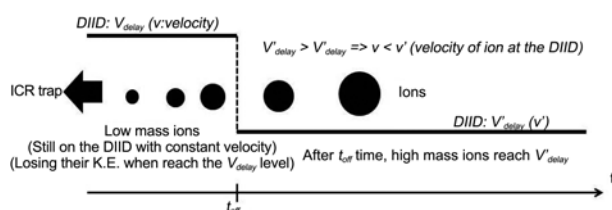


Figure 3. Control scheme of V_{delay} and t_{off} .

if V_{delay} is changed over time, then it can cause overlap to occur. Additionally, t_{off} determines the overlap boundary dividing low- and high-mass ions.

Simulation Results

To investigate the spatial distribution of ions in the ICR trap, ion-trajectory simulations were carried out with SIMION Version 8 software (Scientific Instrument Service Co, Inc. Indianapolis, IN.) on a 3.1 GHz \times 64-based PC with 8 GB RAM. Because the octopole ion guide, DIID, and ICR traps are composed of fine structures and are 1184 mm in length, a single SIMION model could not be used. Therefore, the overall model was separated into three parts: models 1, 2, and 3.

As shown in Figure 4, model 1 included the extraction lens of the collision cell and the octopole ion guide, model 2 included gap 2, and model 3 included the DIID and the ICR trap. As shown in Figure 1(a), the DIID was installed in a 154-mm space between the octopole ion guide and the ICR trap in the KBSI FT-ICR MS.

In model 1, the real octopole ion guide is \sim 1184 mm long. Its spatial size caused a memory problem in the SIMION code because the maximum supported memory was exceeded. To solve this problem, z -positions (injection direction) for which the variation did not affect the potential field (z -symmetry) were used in model 1 to shrink the length of the octopole ion guide. The results of model 1, including velocity, ion position, and time, were used as initial conditions for model 2 in order to synchronize ion movement. The rf field in the octopole ion guide was operated continuously; therefore, only the time value was needed to synchronize the rf fields of models 1 and 2. Model 2 represents gap 2, between the octopole ion guide and the DIID. The DIID consists of a 150-mm-long stacked ring electrode array. In this simulation, we applied a single voltage to each electrode to simplification operation. To calculate the field and ion motion more precisely, a small grid size (0.03175 mm/gu) was used in model 2. The final results of model 2 were used as initial conditions for model 3 to synchronize and integrate the three models into a single, larger model. To help facilitate this, a single potential value was applied at the stacked ring type DIID. Additionally, the DIID within model 3 could be made of a single cylinder electrode because the DIID needs to apply a flat potential field.

First, T vs z plots for each ion mass were calculated using model 3, which was based on calculations from model 1. V_c , the offset voltage of the collision cell of model 1, controlled

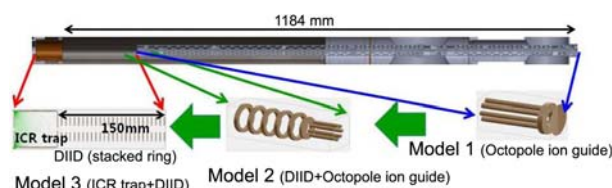


Figure 4. Divided SIMION models for the octopole ion guide, DIID, and ICR trap.

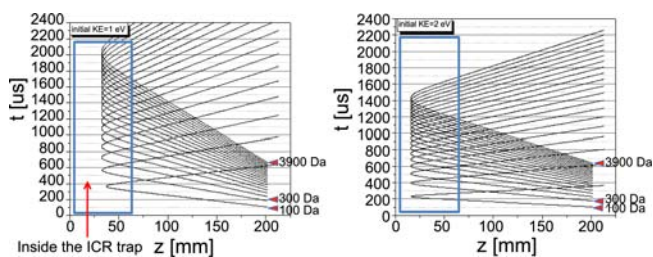


Figure 5. Ion z -position vs time-of-flight for model 3 with ion masses of 100, 300, 500 3900 Da. The initial kinetic energy for model 1 was (a) $V_c = 1$ eV, (b) $V_c = 2$ eV.

the net kinetic energy at the ICR trap. V_c was set to 1.0, and 2 V.

In Figure 5, the square box denotes the area inside the ICR trap; the ion spatial distribution can be compared. The time difference between each ion mass decreased as V_c increased, but this does not mean that the spatial differences decreased. As shown in Figure 5, this effect was due to increased velocity, and the spatial differences actually increased. The turning position of each ion mass in the ICR trap is also important. The ICR trap is a cylindrical, closed trap, and ground voltage was applied at all electrodes, except for the back trap plate. Thus, there was a potential gradient near the back trap plate. As an ion kinetic energy increases, its turning position inside the ICR trap will approach the back trap plate. Gated trapping can increase the trapping mass range. However, if the ion kinetic energy (V_c) increases, the trap voltage of the ICR trap plate must also be increased, thus decreasing the mass resolution¹. We set $V_c = 2.0$ V, which is a typical value for V_c . The resulting plot was used to estimate the mass-detection range for gated trapping. V_c , V_{offset} , and V_{delay} were set to 2.0, -60, and 0 V, respectively. Figure 5(b) shows the mass range trapped when the ICR trap was closed at 1200 μ s (trace of the $t = 1200$ μ s line), which ranged from 1500 to 2900 Da. To measure lighter ions, the closing time t must be shorter than 1200 μ s. A trace of the $t = 600$ μ s line indicates that the mass range was only 500-900 Da. Thus, to measure lighter ions, the mass-detection range should be lowered. Next, we changed the voltage of the DIID (V_{delay}). As shown in Figure 6, we set $t_{off} = 350$ μ s based on Figure 5(b).

This created a boundary near 1300 Da, which divided high-mass and low-mass ions. Before t_{off} , V_{delay} was set to a positive voltage (e.g., 0.78, 0.82 V), t_{off} , V_{delay} was set to 0 V. In this case, the effective kinetic energy of an ion for model 3 was estimated as $V_c V_{delay}$. If V_c is constant, increasing V_{delay} will decrease the effective kinetic energy of ions. Figure 6 shows the deceleration of light ions (red dotted line); the velocity of high-mass ions (black solid line) was unchanged. However, as V_{delay} increased, the decelerated light ions lost energy and could not pass through the potential gradient of the ICR trap. Therefore, the turning positions of decelerated ions receded from inside the ICR trap. To solve this problem, V_{delay} was modified. Before t_{off} , V_{delay} was set to 0.78, 0.82 V, but after t_{off} , V_{delay} was set to voltages greater than zero, such as 0.2 and 0.5 V. These low voltages after t_{off} correspond to

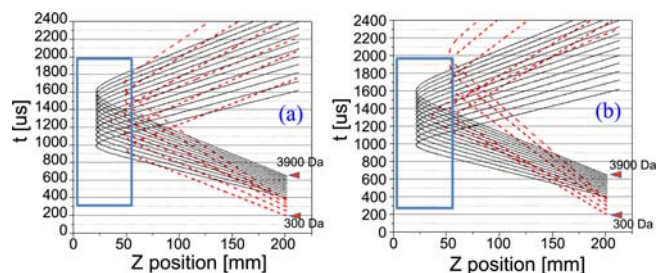


Figure 6. $V_c = 1.5$ eV, $t_{off} = 350$ μ s, low-mass boundary was set near 1300 Da. (a) $V_{delay} = 0.78$ V, (b) $V_{delay} = 0.82$ V.

increased kinetic energy. When ions exit the DIID at $V_{delay} = 0.5$ V, they accelerate because most of the electrodes in the ICR trap had an applied voltage of zero (except for the back trap plate) at that time. In this case, the velocity of high-mass ions also changed due to low voltage; after t_{off} , high-mass ions were also delayed by V_{delay} at that time. Therefore, if we apply voltages greater than zero after t_{off} , high-mass ions will also be slightly decelerated and delayed. The potential level and gradient in most of the ICR trap is almost zero; therefore, small variations in kinetic energy can move the turning position of ions to deep inside the ICR trap.

Figure 7 shows that the overlap between low- and high-mass ions can be controlled, and low-mass ions can travel far into the ICR trap. If the ICR trap is closed at $t = 1500$ μ s (gated trapping), the mass ranges of trapped ions will be \sim 700-1100 Da and 1500-3000 Da (Figure 7(b)). Figure 8(a) shows KE at the z -position without the DIID in operation.

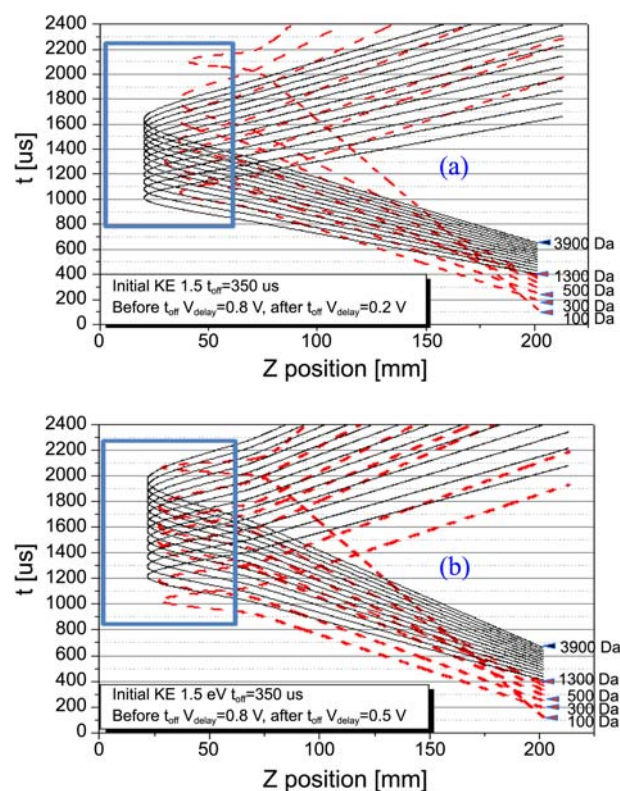


Figure 7. Initial kinetic energy = 1.5 eV, $t_{off} = 350$ μ s. Before t_{off} , $V_{delay} = 0.8$ V. After t_{off} , V_{delay} was changed to 0.2 V and 0.5 V.

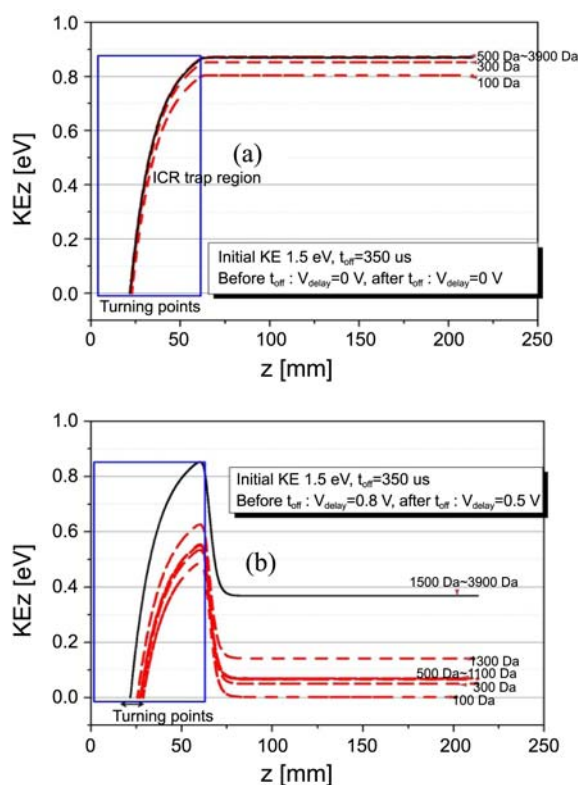


Figure 8. z-position vs KE plot (a) Initial kinetic energy = 1.5 eV, $t_{off} = \infty$, $V_{delay} = 0.8$ V (Figure 5(b)) (b) Initial kinetic energy = 1.5 eV, $t_{off} = 350$ μ s. Before t_{off} , $V_{delay} = 0.8$ V. After t_{off} , $V_{delay} = 0.5$ V.

Figure 8(b) shows that the kinetic energy of lighter ions (100 Da-1300 Da) decelerated upon application of 0.8 V before the t_{off} finish time. After the t_{off} time, 0 V is applied to the DIID, when ions can be decelerated by the electrostatic field, but cannot go into the ICR trap. Their “turning point” in ICR trap is spread out. To reduce the spatial difference of turning points, 0.5 V is applied to the DIID after the t_{off} time to change the KE of ions (100 Da-1300 Da). The spatial distribution between low- and high-mass ions in the ICR trap can be improved using a DIID under optimized conditions.

Conclusion

In the ICR trap, the spatial distribution between low-mass and high-mass ions can be improved using a DIID under optimized conditions. From the results, we confirm that the DIID can be operated as control optics for ion’s spatial focusing. Of course, the SIMION code cannot evaluate collective scattering effect by residual molecular or the space charge effect efficiently. Therefore, experiments will be performed. We presented simulation results for optimal DIID operation conditions and optimized the control parameters (t_{off} , V_{delay}) to minimize the spatial distribution of ions in FT-ICR MS using SIMION.

Acknowledgments. This work was supported by the Korea Basic Science Institute.

References

1. Marshall, A. G.; Hendricson, C. L.; Jackson, G. S. *Mass Spectrum. Review* **1998**, *17*, 1.
2. Choi, M. C.; Park, K. H.; Kim, S. W.; Yoo, J. S.; Kim, H. S. *Rapid Comm. Mass Spectrom.* **2010**, *24*, 469.
3. Dey, M.; Castoro, J. A.; Wilkins, C. L. *Anal. Chem.* **1995**, *67*, 1575.
4. Kaiser, N. K.; Skulason, G. E.; Weisbrod, C. R.; Bruce, J. E. *J. Am. Soc. Mass Spectrom.* **2009**, *20*, 755.
5. Hofstadler, S. A.; Laude, D. A., Jr. *Int. J. Mass Spectrom. Ion Processes* **1990**, *101*, 65.
6. Castoro, J. A.; Koster, C.; Wilkins, C. L. *Rapid Commun. Mass Spectrom.* **1992**, *6*, 239.
7. Knobeler, M.; Wanczek, K. P. *Int. J. Mass Spectrom. Ion Processes* **1997**, *163*, 47.
8. Gooden, J. K.; Rampel, D. L.; Gross, M. L. *J. Am. Soc. Mass Spectrom.* **2004**, *15*, 1109.
9. Rempel, D. L.; Gross, M. L. *J. Am. Soc. Mass Spectrom.* **2001**, *12*, 296.
10. Frankevich, V.; Zenobi, R. *Rapid Commun. Mass Spectrom.* **2001**, *15*, 2035.
11. Frankevich, V.; Zenobi, R. *Rapid Commun. Mass Spectrom.* **2001**, *15*, 979.
12. Tosi, P.; Fontana, G.; Longano, S.; Bassi, D. *Int. J. Mass Spectrom. Ion Processes* **1989**, *93*, 95.
13. Guan, S.; Marshall, A. G. *Int. J. Mass Spectrom. Ion Processes* **1995**, *146/147*, 261.